Zooming into π-Stacked Manifolds of Nucleobases: Ionized States of Dimethylated Uracil Dimers

Anna A. Zadorozhnaya and Anna I. Krylov*

Department of Chemistry, University of Southern California, Los Angeles, California 90089-0482

Received: November 2, 2009; Revised Manuscript Received: December 17, 2009

The electronic structure of 1,3-dimethyluracil and its dimer is characterized by *ab initio* calculations. The methylation eliminates the H-bonded isomers and allows one to focus on the π-stacked manifold. In the neutral species, methylation increases the binding energy by 3−4 kcal/mol and reduces the lowest ionization energy (IE) by 0.6 eV. Other valence IEs are also red-shifted and the relative state ordering is the same as in uracil; however, the magnitude of the effect varies from 0.37 to 0.86 eV. The largest shifts are observed for the states with large contributions from lone pairs of nitrogens, which are primary substitution sites. The effect of stacking interactions on IEs is similar in methylated and non-methylated dimers: the lowest IE is red-shifted by 0.37 and 0.35 eV relative to the respective monomers. The splittings between other pairs of dimer states derived from the in-phase and out-of-phase combinations of the monomers' states are also similar to non-methylated uracil dimers, except for the states that include a large weight of nitrogen lone pairs. Because of the nonuniform effect on both monomers' levels and the shifts, the relative order of the ionized states in the dimer changes, relative to that of the non-methylated uracil dimer. The ionized stacked isomers show two different relaxation patterns—several isomers form structures with the delocalized hole stabilized by the orbital overlap, whereas others relax to the structures with the localized hole stabilized by electrostatic interactions. Electronic spectra of the ionized species at the neutral and cation geometries are presented and discussed.

1. Introduction

Gas-phase clusters of nucleobases play an important role as model systems for studying properties of DNA.[1–5] Owing to their small size, high-level computational methods can be applied to obtain an accurate and detailed description of their electronic structure. The theoretical predictions can be tested by gas-phase experiments. These studies, which allow us to focus on the intrinsic properties of DNA's building blocks and their interactions,[5] are a prerequisite for investigating the effects of more complex environments (backbone, counterions, solvent, etc.) on the properties of these molecules. Moreover, they provide benchmark data for calibrating more approximate computational methods that can tackle larger systems. Also, new experimental techniques can be probed and developed using these small model systems.

Recently, we characterized the electronic structure of the ionized uracil dimers,[6,7] adenine and thymine homo- and heterodimers,[8] and cytosine dimers.[9] Calculations[6–9] and VUV measurements[8,9] demonstrated that noncovalent interactions lower vertical ionization energies (VIEs) by as much as 0.7 eV (in cytosine dimers). Interestingly, the magnitude and origin of the effect are different for different isomers. The largest drop in IEs was observed in the symmetric stacked and nonsymmetric H-bonded dimers. In the former case, the IE is lowered due to the hole delocalization over the two fragments and the change depends on the overlap between the fragments' molecular orbitals (MOs). In the latter case, the overlap does not play an important role—the hole, which is localized on one of the fragments, is stabilized by the electrostatic interactions with the "neutral" fragment. In this case, the magnitude of the IE drop is determined by the magnitude and orientation of the dipole moment of the spectator fragment. The changes of IEs due to H-bonding in the symmetric H-bonded dimers were found to be smaller.[8,9] Because cytosine and thymine are more polar than adenine, their dimers (both stacked and H-bonded) exhibit larger shifts than the dimers of adenine. Thus, noncovalent interactions seem to reduce the gaps in IEs of purines and pyrimidines, which may play an important role in hole migration through DNA.

Comparison of the computed IEs for different isomers with the experimental photoionization efficiency curves suggested that multiple isomers are present in the beam prepared by thermal desorption,[8,9] in agreement with previous experimental and computational studies.[2,3,10] Numerous isomers of the gas-phase dimers and their nonthermal populations complicate the interpretation of experimental measurements. One can reduce the number of isomers by using methylated species that do not form H-bonded dimers.[11–14] By removing the entire H-bonded manifold, one can zoom into stacked isomers representing a π-stacking structural motif so prominently present in DNA. However, methylation may affect the monomer's properties,[15,16] and also change the interactions in the stacked dimers. Thus, it is important to quantify the differences between methylated species and their non-methylated analogues.

Our studies of uracil dimers[6,7] focused on their electronic spectroscopy, which may be used to discriminate between the isomers and to monitor ionization-induced dynamics. For example, π-stacked isomers feature intense charge-resonance (CR) bands, which are very sensitive to the relative orientation of the fragments and the overlap of the fragments' molecular orbitals (FMOs).[17–24] In the lowest-energy π-stacked isomer of the uracil dimer, the CR band appears at 0.52 eV at the geometry of the neutral dimer, and shifts to 1.25 eV upon structural relaxation of the cation. The symmetric H-bonded isomers have less intense CR bands at lower energies, and they disappear

10.1021/jp910440d
Published on Web 01/07/2010

upon ionization-induced proton transfer.[6,7] The t-shaped isomer features higher-energy bands corresponding to charge-transfer transitions.

The goal of this work is to characterize the electronic structure of the lowest-energy methylated uracil dimers. We discuss the structures and binding energies of the several lowest neutral isomers. The structural relaxation in the ionized systems and the binding energies of the cations are also presented. We investigate the effect of methylation on the ionized states of the monomer and dimers, and quantify the changes in IEs due to π-stacking interactions. As the results below demonstrate, the methylation results in nonuniform red shifts in the monomer's levels, and also affects the magnitude of the splittings between the dimer states, resulting in a different state ordering in the dimer. Finally, we present electronic spectra calculations for the lowest-energy methylated dimer. As in the case of non-methylated species, the hole delocalization gives rise to the intense CR band characteristic of the ionized dimer.

2. Theoretical Methods and Computational Details

Electronic structure calculations of dimer cations are challenging owing to the open-shell character of these species, as discussed in detail in our previous studies.[6–8,21,25] The common problems include symmetry breaking, spin-contamination, and inverse symmetry breaking due to self-interaction error.

Within the wave function formalism, these systems are best described by the equation-of-motion coupled-cluster method for ionization potentials, EOM-IP-CCSD or simply IP-CCSD,[22,26–29] and by its less expensive configuration interaction approximation, IP-CISD.[30] EOM-IP-CCSD and IP-CISD describe problematic doublet wave functions as ionized states derived from a well-behaved closed-shell wave function; i.e., the target open-shell wave functions are generated by a Koopmans-like excitation operator R acting on the reference wave function:

$$\Psi^{\mathrm{EOM-IP}}(N-1) = \hat{R}\Psi_0(N) \qquad (1)$$

where $\Psi_0(N)$ is the wave function of the N-electron neutral system and R consists of $1h$ and $2h1p$ (1 hole and 2 hole 1 particle, respectively) operators generating $(N-1)$-electron determinants from the N-electron reference. In the more accurate IP-CCSD method, Ψ_0 is a correlated CCSD wave function, whereas Ψ_0 in IP-CISD is just a single Slater determinant. Amplitudes of R are found by diagonalization of the similarity-transformed (IP-CCSD) or bare (IP-CISD) Hamiltonian.

In DFT methods, self-interaction error can be mitigated by including long-range Hartree−Fock exchange.[31–33] We employed the ωB97X-D functional,[34] which also includes empirical dispersion terms.[35]

In this study, we employed a variety of *ab initio* techniques. The structures were obtained as follows. For the monomer, we employed the RI-MP2/cc-pVTZ and IP-CISD/6-31(+)G* methods[36,37] in the neutral and the cation optimizations, respectively. Different starting geometries were used in optimizations including the C_s and C_1 conformers with different angles of rotation of the CH_3 groups. We found that both the neutral and the ionized 1,3-dimethyluracil have C_s structures in which only the hydrogens of the CH_3 groups lie out of plane.

By considering the two main factors contributing to the stability of the stacked dimers, i.e., electrostatic interactions and steric repulsion, five starting geometries were generated for the optimization, which employed a DFT-D method with the ωB97X-D functional,[34] the 6-311(+,+)G(2d,2p) basis set,[38] and the EML(75,302) grid. The basis set and grid combination was chosen based on the numerical tests, which showed that calculations with smaller bases, e.g., 6-311(+,+)G**, and smaller grids fail to reproduce the degeneracy of enantiomeric structures. Tight convergence criteria were enforced in all optimizations, with the gradient and energy tolerance set to 3×10^{-5} and 1.2×10^{-4}, respectively, and the maximum energy change 1×10^{-7}. For the only symmetric isomer, we carried out additional optimization without the symmetry constraint, which proved that the minimum-energy structure is indeed C_i symmetric.

The same level of theory was used in the dimer cation optimizations. We used the neutral structures as the starting geometries. All cation optimizations employed the spin-unrestricted references. The spin-contamination of the doublet Kohn−Sham determinant was low with the typical $\langle S^2 \rangle$ values within the 0.76−0.77 range. Just like in the neutrals, the C_i symmetry of the only symmetric isomer was tested by additional optimizations without the C_i constraint.

The dissociation and ionization energies and the electronic spectra of the cations were then calculated with the IP-CCSD method and a moderate 6-31(+)G* basis set. In the monomer calculations, we also employed a larger 6-311(+)G** basis to investigate the basis set effect on ionization energies. Core electrons were frozen in the single-point IP-CCSD energy and spectra calculations.

Optimized geometries, relevant total energies, and harmonic frequencies are given in the Supporting Information. The data on the non-methylated uracil monomer and dimer to which we frequently refer in this work are from refs 6 and 7. All calculations were performed using the *Q-CHEM* electronic structure program.[39]

3. Results and Discussion

3.1. Potential Energy Surface of the Neutral Dimers: Structures and Energetics. Nucleobase dimers form numerous isomers,[2,3,10] which can be described as the stacked, t-shaped, and H-bonded structures. Three representative isomers from each manifold have been characterized in our recent study of the uracil dimer.[7] The H-bonded structure corresponds to the global energy minimum in non-methylated species.

Methylation at nitrogens reduces the polarity of the molecule, eliminates hydrogens that can participate in H-bonding, and introduces bulky groups. These factors destabilize the t-shaped and H-bonded structures of the 1,3-dimethyluracil dimers. The molecular dynamics study by Hobza and co-workers[11] showed that the potential energy surface (PES) of the 1,3-dimethyluracil dimers is dominated by the stacked structures, the t-shaped isomers lying 5−6 kcal/mol higher in energy and H-bonded isomers being unstable. Our calculations using ωB97X-D/6-311(+)G** found a H-bonded-like structure (which is better described as a van der Waals dimer) about 10 kcal/mol above the stacked manifold. Thus, we focus on the stacked isomers of the 1,3-dimethyluracil dimer.

The five optimized structures of the neutral stacked 1,3-dimethyluracil are shown in Figure 1; the corresponding binding and relative energies calculated with ωB97X-D/6-311(+,+)G(2d,2p) and CCSD/6-31(+)G* are summarized in Tables 1 and 2, respectively.

The lowest-energy structure of the dimethylated uracil dimer is nonsymmetric isomer 1, which is similar to the minimum-energy stacked uracil structure from the S22 set by Hobza and co-workers.[40] This isomer is followed by isomers 2 (C_i), 3 (C_1), 4 (C_1), and 5 (C_1) lying 1.2, 1.5, 2.2, and 2.9 kcal/mol higher

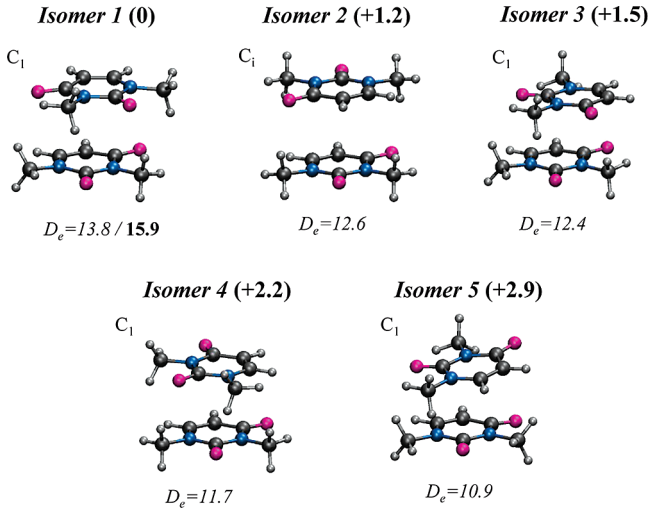

Figure 1. Five isomers of the stacked neutral 1,3-dimethyluracil dimer and their binding energies (kcal/mol). The energy spacings (kcal/mol) between the lowest-energy structure and other isomers are given in parentheses. All values were obtained with ωB97X-D/6-311(+,+)G(2d,2p)/EML(75,302) except for the D_e value of isomer 1 shown in bold, which is the IP-CCSD/6-31(+)G* estimate.

TABLE 1: Total (hartree) and Dissociation Energies (kcal/mol) of the Neutral and Ionized 1,3-Dimethyluracil Monomer and Dimers Calculated at the ωB97X-D/6-311(+,+)G(2d,2p)/EML(75,302) Level of Theory

complex	E^{tot}_{DFT-D}	D_e^{DFT-D}
mU^0	−493.431022	
mU^+	−493.111429	
$S(mU)_2^0$, isomer 1	−986.884084	13.8
$S(mU)_2^0$, isomer 2	−986.882142	12.6
$S(mU)_2^0$, isomer 3	−986.881741	12.4
$S(mU)_2^0$, isomer 4	−986.880611	11.7
$S(mU)_2^0$, isomer 5	−986.879409	10.9
$S(mU)_2^+$, isomer 1	−986.587029	28.0
$S(mU)_2^+$, isomer 2	−986.570893	17.9
$S(mU)_2^+$, isomer 3	−986.578185	22.4
$S(mU)_2^+$, isomer 4	−986.576570	21.4
$T(mU)_2^+$, isomer 5	−986.572944	19.1

TABLE 2: Total (hartree) and Dissociation Energies (kcal/mol) of the Neutral and Ionized 1,3-Dimethyluracil and Its Dimer (Lowest-Energy Isomer) Calculated at the IP-CCSD/6-31(+)G* Level of Theory[a]

complex	E^{tot}_{CCSD}	D_e^{CCSD}	ΔE^{CCSD}_{relax}
mU^0	−492.032033		
mU^+	−491.715681		−3.8
$S(mU)_2^0$, isomer 1	−984.089466	15.9	
$S(mU)_2^+$, isomer 1	−983.798612	31.9	−11.2
U^0	−413.683919		
U^+	−413.345482		−4.1
SU_2^0	−827.387312	12.2	
SU_2^+	−827.069011	24.9	−8.7

[a] For the monomer and dimer cations, the relaxation energy (ΔE^{CCSD}_{relax}, kcal/mol) is provided (the difference between the total energies of the cation at the vertical and relaxed geometries). The uracil and uracil dimer IP-CCSD/6-31(+)G* results are included for comparison. (For these estimates, we employed the same structures as those in ref 7. For the stacked uracil dimer cation, the DFT-D/ωB97X-D/6-311(+)G** optimized geometry was used.)

in energy, respectively. The energy gaps between the isomers are very small: the five isomers lie in just the 2.9 kcal/mol range, and some of them are nearly degenerate, i.e., separated by 0.3 kcal/mol. These energy differences are of the order of kT(298.18 K) = 0.6 kcal/mol, which suggests significant populations of all of these isomers at the standard laboratory conditions. The dense π-stacked manifold and structural motifs are similar to stacked thymine dimers,[8] where five isomers lie within 2.2 kcal/mol. Interestingly, no low-energy stacked isomers were identified for dimers of another pyrimidine, cytosine dimer.[9]

The binding energies of the neutral stacked 1,3-dimethyluracil dimers lie in the range 10.9−13.8 kcal/mol, as computed by DFT-D. For the lowest-energy isomer, we also computed the CCSD/6-31(+)G* value. The resulting binding energy of 15.9 kcal/mol is in good agreement with 13.8 kcal/mol computed with ωB97X-D/6-311(+)G**. On the basis of our results for uracil,[7] using a larger basis set in CCSD calculations lowers the CCSD binding energy and improves the agreement between the methods.

The binding energy of the lowest-energy isomer (13.8 kcal/mol) is larger than that of the stacked non-methylated uracil dimer for which D_e = 10.5 kcal/mol (these are DFT-D values, but a similar trend is observed for the CCSD/6-31+G* binding energies, which are 15.9 and 12.2 kcal/mol). For comparison, the binding energies of the lowest stacked thymine and adenine homodimers are 12.5 and 10.6 kcal/mol, respectively.[8]

An increase in binding energy upon methylation is somewhat surprising, as methylated uracil is less polar than uracil (the RI-MP2/cc-pVTZ dipole moments are 4.19 D versus 4.02 D), and therefore, one may expect weaker electrostatic interaction between the fragments in the 1,3-dimethyluracil dimer. However, this difference appears to be too small, and local electrostatic interactions play a more important role. The analysis of the structures reveals that the $(NCH_2)H^{\delta+}\cdots O^{\delta-}(C)$ distance in the stacked 1,3-dimethyluracil dimer is shorter than the $(N)H^{\delta+}\cdots O^{\delta-}$ distance in the stacked uracil dimer, which results in stronger electrostatic interaction between the fragments in the former complex. A tighter structure of the methylated dimer is also counterintuitive because of the presence of the bulky methyl groups. The observed increase in binding energy upon substitution is consistent with the results of Sherrill and co-workers,[41,42] who demonstrated that the electrostatic considerations alone are not sufficient to explain the changes in binding in π-stacked systems upon substitution and that differential changes in dispersion interactions play an important role.

3.2. Effect of Methylation on the Ionized States of the Monomer and the Dimers. ***3.2.1. 1,3-Dimethyluracil.*** Figure 2 presents the five highest occupied MOs of 1,3-dimethyluracil and uracil and the corresponding VIEs calculated at the IP-CCSD/6-311(+)G** level.

The shapes of the MOs are similar in the two molecules, except for the σ_{CH} electronic density on the CH_3 groups of 1,3-dimethyluracil. Another minor difference can be seen in the lp(N) + π_{CC} + π_{CO} orbital, which is more localized in dimethylated uracil.

The order of the ionized states in methylated uracil is the same as that in uracil. The HOMO is the π-like MO centered at the C−C double bond, and the corresponding IE is 8.87 eV. This state is followed by ionization from the two lone pair and two π-like orbitals with VIEs of 9.74 (lp(O_1)), 9.77 (lp(O) + lp(N)), 10.66 (lp(O_2)), and 12.16 eV (lp(N) + π_{CC} + π_{CO}).

However, the values of IEs and the spacings between the ionized states are different. Methylation lowers the first IE by 0.6 eV relative to uracil. A similar effect is observed for other states: the VIEs of the $1^2A'$, $1^2A''$, $2^2A'$, and $2^2A''$ states decrease by 0.37, 0.74, 0.43, and 0.86 eV, respectively. Note that, for the oxygen lone-pair states, the magnitude of the effect is smaller than that for the states derived from ionization from π-like

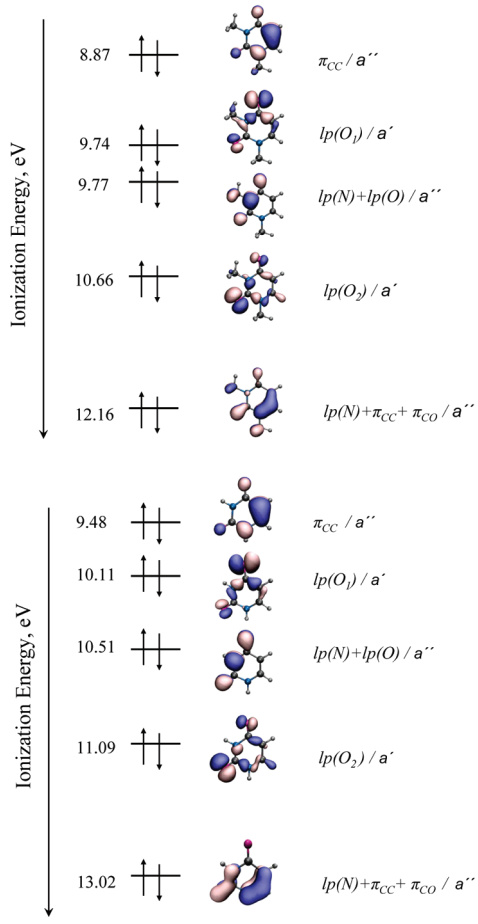

Figure 2. The five lowest ionized states and the molecular orbitals of 1,3-dimethyluracil (top) and uracil (bottom) calculated by IP-CCSD/6-311(+)G**.

orbitals. The largest shifts are observed for the states with large contributions from lone pairs of nitrogens, which are primary substitution sites. As a result, the $1^2A'$ and $1^2A''$ states that are separated by 0.4 eV in uracil become almost degenerate in 1,3-dimethyluracil.

The IEs are lowered due to electron-donating CH_3 groups increasing the electron density in the ring (destabilization of the respective MOs) and due to a larger size of the methylated species contributing to hole stabilization. The effect is larger in the states derived from ionization from delocalized π-orbitals, in which the CH_3 group donates the electron density to the π-system via the lp(N) component, whereas the in-plane lp(O) orbitals are affected less.

3.2.2. Dimethyluracil Dimers. Similarly to other π-stacked dimers,[6–8,21] the electronic structure and ionized states of the 1,3-dimethyluracil dimer can be described within the DMO-LCFMO framework.[21] The molecular orbitals of the dimer (DMOs) shown in Figure 3 are the in- and out-of-phase combinations of the FMOs. Figure 3 also presents the corresponding IEs. Because of the lower symmetry, some of the electronic states of the methylated uracil dimer are localized on individual fragments.

The first IE of the 1,3-dimethyluracil dimer corresponds to ionization from the π_{CC}(F1)−π_{CC}(F2) DMO. Stacking interaction lowers it by 0.37 eV relative to the monomer, i.e, 8.40 eV versus 8.77 eV, as calculated at the IP-CCSD/6-31(+)G* level. Thus, the magnitude of the effect is comparable to that in the non-methylated stacked uracil dimer and the stacked thymine dimer (both have 0.35 eV decrease in IE), whereas the shift in adenine dimer is smaller (0.2 eV).[8]

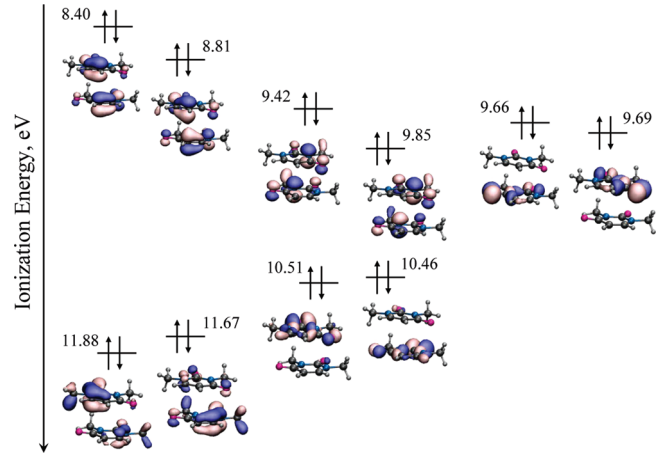

Figure 3. The 10 lowest ionized states and the corresponding MOs of the lowest-energy isomer of neutral stacked 1,3-dimethyluracil computed with IP-CCSD/6-31(+)G*.

The order of the ionized states in the 1,3-dimethyluracil dimer is different from the uracil dimer. In the latter (as well as in the stacked thymine dimer, see ref 8), the states corresponding to the in- and out-of-phase FMO combinations appear pair by pair in the same order as the respective monomer states. In the methylated uracil dimer, the states arising from ionization from $lp(O_1)$ FMOs lie in between the pair of states corresponding to the lp(O) + lp(N) FMOs.

The largest splittings between the pairs of states are observed for the states derived from the π-like FMOs owing to their larger overlap. Compare, for example, the 0.41, 0.43, and 0.21 eV splittings for the states derived from ionization from the π-like orbitals to the 0.06 and 0.05 eV splittings for the lone-pair states. Overall, the magnitude of the splittings in methylated and non-methylated dimers is similar, except for the lp(O) + lp(N) pair of states (0.43 eV vs 0.06 eV in the 1,3-dimethyluracil and uracil dimers, respectively). Due to the large weight of lp(N), these MOs are most affected by the electron-donating CH_3 groups. The increased electron density in the π-system results in larger overlap and, consequently, larger splittings. This large splitting is responsible for different state ordering. So far, this is the first example of that type—in all other model systems we have studied (benzene, uracil, and adenine dimers), the stacking interactions did not change the relative order of the ionized states, even though the splittings in different pairs of states were quite different.

3.3. Ionization-Induced Changes in the Monomer and the Dimers: Structures and Properties. Ionization induces considerable structural changes. For the lowest ionized state, the relaxation pattern is consistent with the MO character. In the uracil monomer, the double CC bond elongates, inducing the changes in an entire bond-alternation pattern.[7] In the dimer, these changes are accompanied by the rings reorienting to increase the overlap between the respective FMOs.[7] Methylated species show very similar behavior. Below, we discuss changes in binding energies and relative order of the isomers and characterize spectroscopic signatures of the structural relaxation.

3.3.1. Binding Energies of the Dimer Cations. Figure 4 presents five relaxed structures of the 1,3-dimethyluracil dimer cations. The total and dissociation energies of the dimer cations estimated by ωB97X-D are given in Table 1, and the CCSD/6-31(+)G* estimates for the lowest-energy isomer are provided in Table 2.

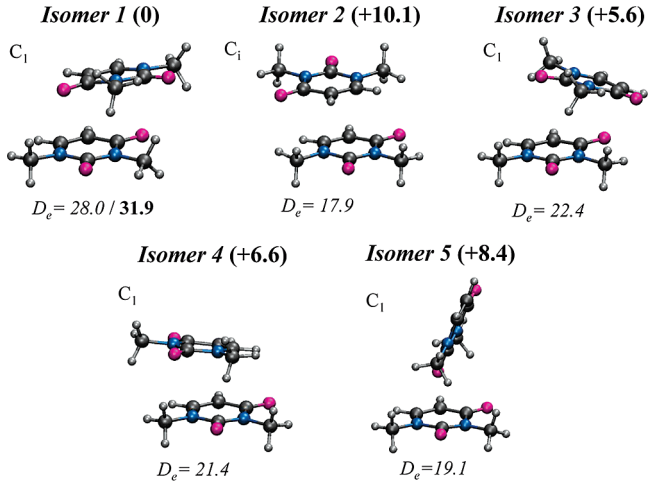

Figure 4. Five low-lying isomers of the 1,3-dimethyluracil dimer cation and the dissociation energies (kcal/mol). The energy spacings (kcal/mol) between the lowest-energy structure and other isomers are given in parentheses. All values were obtained with ωB97X-D/6-311(+,+)G(2d,2p)/EML(75,302) except for the D_e value of isomer 1 (shown in bold), which is the IP-CCSD/6-31(+)G* estimate.

Similarly to the neutral dimers, the global minimum corresponds to isomer 1 (C_1). However, in all other aspects, the PES of the dimer cation differs drastically from that of the neutral.

The order of the isomers and the energy gaps between them change upon ionization. Following isomer 1, isomers 3, 4, 5, and 2 lie 5.6, 6.6, 8.4, and 10.1 kcal/mol higher in energy. In contrast to the neutral, the five minima on the cation PES are well-separated in energy. For example, the two lowest-energy structures are more than 5 kcal/mol apart, whereas all five neutral isomers lie within a 2.9 kcal/mol interval. Thus, we expect a dominant population of the lowest-energy structure (isomer 1) of the cation under the standard conditions. Another difference is the appearance of the t-shaped dimer cation (isomer 5) among low-lying structures. It is 8.4 kcal/mol above isomer 1 (but 1.5 kcal/mol below one of the stacked structures).

The dissociation energies of 1,3-dimethyluracil cations fall within the 17.9−28.0 kcal/mol range, as computed with DFT-D. Therefore, the fragments in ionized dimers are bound 1.4−2.0 times stronger than in the neutral dimers with the largest and the smallest increases observed for isomers 1 and 2, respectively. The magnitude of the increase is similar to that observed in the uracil dimers. Note that, similarly to the neutral dimers, the interaction between the fragments is stronger in the methylated dimers than in the non-methylated analogues. The best estimate of the binding energy for the lowest-energy cation structure (isomer 1) is 31.9 kcal/mol (at the IP-CCSD/6-31(+)G* level), which is 7.0 kcal/mol larger than that of the stacked uracil dimer (24.9 kcal/mol at the IP-CCSD/6-31(+)G* level). The binding energy of the ionized stacked thymine dimer is similar to that of uracil, i.e., 19.8 kcal/mol. The increase of binding energy upon methylation can be explained by the increased electron density in the π-system resulting in a larger overlap, and is consistent with a slightly larger change of IE due to dimerization. Another contribution into the binding energy comes from the geometric relaxation, which is larger in the methylated dimer relative to the non-methylated species (11.2 vs 8.7 kcal/mol). The corresponding relaxation energies in both monomers are about 3−4 kcal/mol (see Table 2). Larger geometric relaxation in the methylated dimer is similar to the results for the stacked thymine and adenine homodimers,[8] where the difference between VIE and AIE was 15.0 and 11.3 kcal/mol for TT and AA, respectively, and the corresponding monomer values were 5−6 kcal/mol.

3.3.2. Equilibrium Geometries of the Cations. The ionization-induced changes in geometry and the electronic structure of isomers 1−5 of the 1,3-dimethyluracil dimer are illustrated in Figures 5−9. In each picture, the neutral and the cation geometries and the two highest MOs of the dimer are shown. The analysis of these five cases reveals two distinct trends. In isomers 1, 2, and 4 (group 1), the relaxation results in the increased FMO overlap and, consequently, the delocalized DMOs at the cation geometry. Isomers 3 and 5 (group 2) exhibit a different pattern: the DMOs are localized on one of the fragments at the cation geometry and no significant FMO overlap develops upon the relaxation. In both structures, lp(O) of one of the fragments moves toward the hole centered on the π_{CC} MO of the other fragment. Thus, group 2 cations are stabilized by the favorable electrostatic interaction of the localized hole and the negative charge on lp(O). This motif, which is similar to the t-shaped uracil dimer,[7] demonstrates that electrostatic interactions can be competitive with the hole delocalization effects even in the stacked systems.

Therefore, two factors are responsible for the stabilization of the ionized 1,3-dimethyluracil dimer cations: the DMO-LCFMO mechanism in which the stabilization of the ionized state is proportional to the FMO overlap[21] and the electrostatic mechanism.[7−9] The magnitude of relaxation is comparable for the two mechanisms; e.g., in group 1, the binding energy increases 1.4−2.0 times relative to the neutrals, and for group 2, the increase is 1.7−1.8-fold. However, one may expect that the DMO-LCFMO stabilization is more sensitive to the relative orientation of the fragments than electrostatic interactions and that the constrained environments (e.g., DNA) may discriminate between the two effects, although it is not clear how strong perturbation by the backbone will affect the relative strengths of these interactions.

Let us now compare the absolute values of the binding energies for isomers 1−5. For the group 1 isomers stabilized via the DMO-LCFMO mechanism, the strongest and weakest interfragment interaction is observed in isomer 1 (28.0 kcal/mol) and symmetric isomer 2 (17.9 kcal/mol), respectively. The difference between these two cases is apparent from Figures 5 and 6. In isomer 1, the DMOs look more like a bonding orbital, whereas isomer 2 fails to develop significant FMO overlap. Isomer 4 (see Figure 8) lies in between these two limiting cases with the moderate overlap and binding energy of 21.4 kcal/mol. In group 2, the values of binding energies are less diverse, which is consistent with the electrostatic stabilization mechanism. In isomers 3 and 5, the fragments are bound by 22.4 and 19.1 kcal/mol, respectively.

3.3.3. Electronic Spectra of the Cations. *1,3-Dimethyluracil.* The electronic spectra of the methylated uracil and uracil cations at the vertical and relaxed geometries calculated by IP-CCSD/6-31(+)* are shown in Figure 10. Table 4 provides the values of transition energies, dipole moments, and oscillator strengths.

Owing to the similarity in their structures and MOs, the spectra of methylated and non-methylated uracil cation are very similar (see Figure 10). In both cases, the two bright transitions correspond to the transitions between the states of the cations with the π-orbitals singly occupied. The methylated uracil spectrum is slightly blue-shifted. The effect of the geometry relaxation on the spectra is larger in the uracil cation than in the 1,3-dimethyluracil cation with line shifts of +0.7−0.8 eV for the former and +0.5−0.6 eV for the latter. This can be

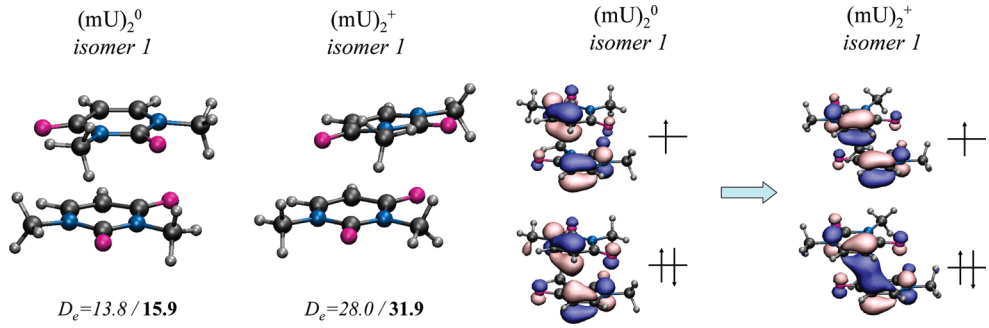

Figure 5. Ionization-induced changes in geometry, binding energies (kcal/mol), and MOs of isomer 1 of the stacked 1,3-dimethyluracil dimer. The ωB97X-D/6-311(+,+)G(2d,2p)/EML(75,302) optimized structures, dissociation energies, and HF/6-31(+)G* MOs are presented.

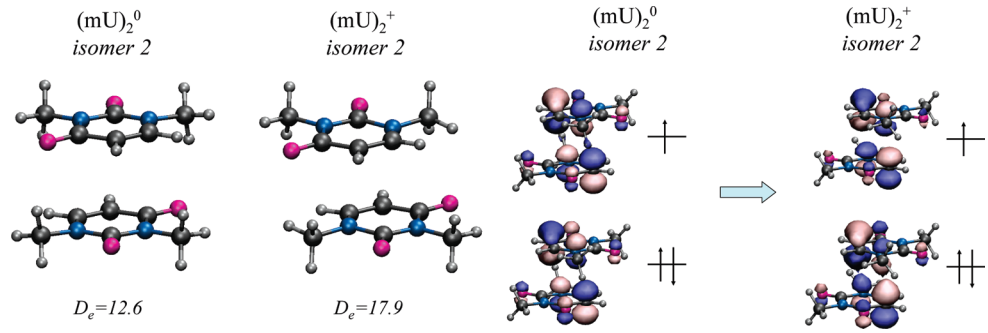

Figure 6. Ionization-induced changes in geometry, binding energies (kcal/mol), and MOs of isomer 2 of the stacked 1,3-dimethyluracil dimer. The ωB97X-D/6-311(+,+)G(2d,2p)/EML(75,302) optimized structures, dissociation energies, and HF/6-31(+)G* MOs are presented.

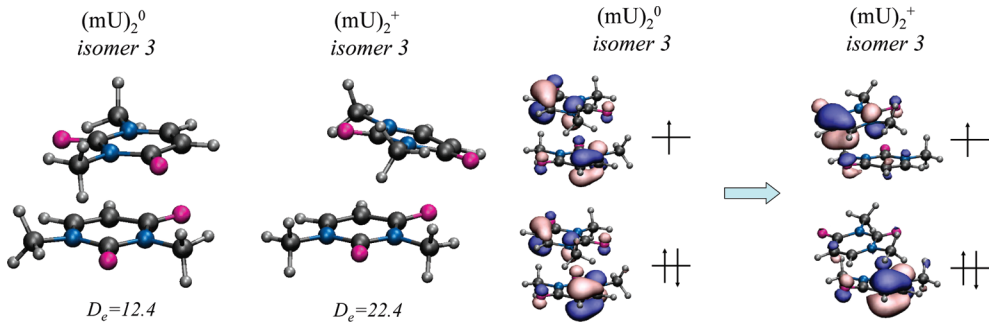

Figure 7. Ionization-induced changes in geometry, binding energies (kcal/mol), and MOs of isomer 3 of the stacked 1,3-dimethyluracil dimer. The ωB97X-D/6-311(+,+)G(2d,2p)/EML(75,302) optimized structures, dissociation energies, and HF/6-31(+)G* MOs are presented.

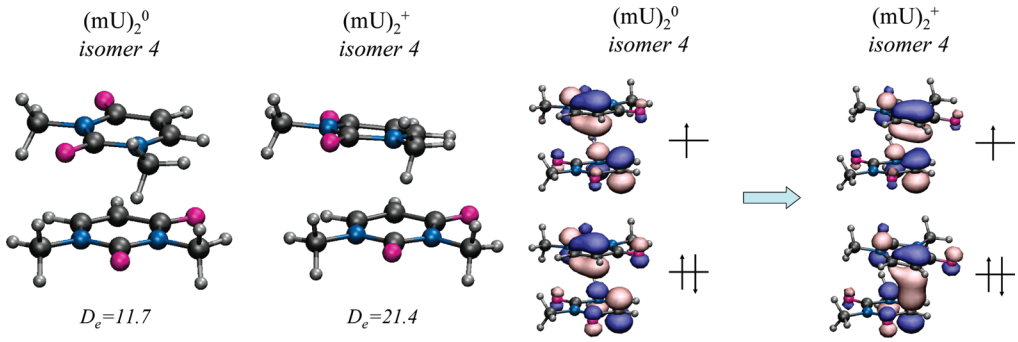

Figure 8. Ionization-induced changes in geometry, binding energies (kcal/mol), and MOs of isomer 4 of the stacked 1,3-dimethyluracil dimer. The ωB97X-D/6-311(+,+)G(2d,2p)/EML(75,302) optimized structures, dissociation energies, and HF/6-31(+)G* MOs are presented.

explained by the electron-donating properties of the CH_3 groups which reduce the effect of ionization on the structure.

1,3-Dimethyluracil Dimer Cation. Table 5 presents IEs of isomer 1 computed at the vertical and relaxed geometries. The respective MOs are shown in Figure 3. Due to the low symmetry and large size of the methylated dimer, we only computed the excitation energies, as calculations of the oscillator strengths for the electronic transitions in the cation are more computationally expensive than just energy calculations. However, the intensities of the peaks can be estimated on the basis of the intensities in the uracil dimer cation[6,7] and DMO-LCFMO analysis (see ref 21 for the DMO-LCFMO nomenclature), as explained below. These results are visualized in Figure 11.

In the stacked uracil dimer cation, the $\psi_-(\pi) \rightarrow \psi_+(\pi)$ and $\psi_-(\pi) \rightarrow \psi_-(\pi)$ transitions (i.e., the transitions between the electronic states derived from the ionization from the DMOs

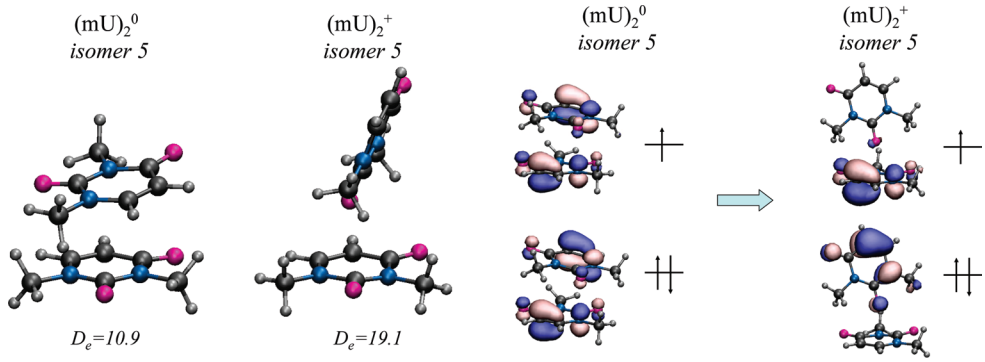

Figure 9. Changes in geometry, binding energies (kcal/mol), and MOs of isomer 5 of the stacked 1,3-dimethyluracil dimer at ionization. The ωB97X-D/6-311(+,+)G(2d,2p)/EML(75,302) optimized structures, dissociation energies, and HF/6-31(+)G* MOs are presented.

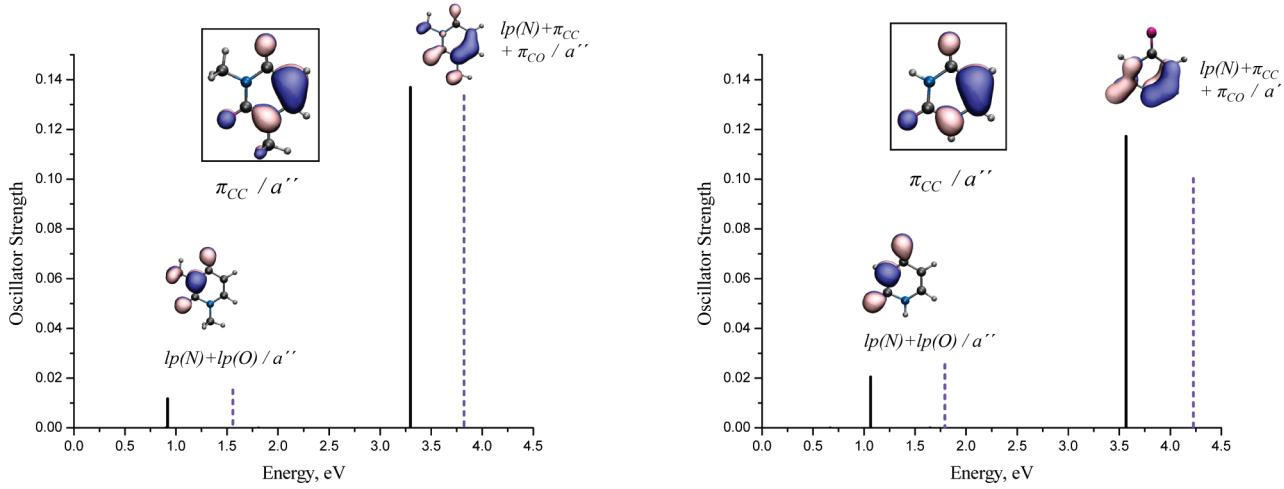

Figure 10. Electronic spectra of 1,3-dimethyluracil (left) and uracil (right) at the vertical (solid black) and relaxed (dashed blue) geometries calculated by IP-CCSD/6-31(+)G*.

TABLE 3: The Five Lowest Ionized States and the Corresponding IEs (eV) of the 1,3-Dimethyluracil at the Vertical Geometry Calculated by IP-CCSD with the 6-31(+)G* and 6-311(+)G Bases[a]**

basis	X^2A''	$1^2A'$	$1^2A''$	$2^2A'$	$2^2A''$
6-31(+)G*	8.77 (−0.61)	9.67 (−0.38)	9.69 (−0.75)	10.58 (−0.45)	12.07 (−0.88)
6-311(+)G**	8.87 (−0.61)	9.74 (−0.37)	9.77 (−0.74)	10.66 (−0.43)	12.16 (−0.86)

[a] The IE shifts (eV) with respect to the uracil values are given in parentheses.

TABLE 4: Electronic Spectrum of the 1,3-Dimethyluracil Cation at the Vertical and Relaxed Geometries Calculated at the IP-CCSD/6-31(+)G* Level

	neutral			cation		
transition	ΔE, eV	$\langle\mu^2\rangle$, au	f	ΔE, eV	$\langle\mu^2\rangle$, au	f
$X^2A'' \rightarrow 1^2A'$	0.899	0.0004	0.0000	1.269	0.0004	0.0000
$X^2A'' \rightarrow 1^2A''$	0.917	0.5222	0.0117	1.557	0.3996	0.0152
$X^2A'' \rightarrow 2^2A'$	1.809	0.0000	0.0000	2.399	0.0000	0.0000
$X^2A'' \rightarrow 2^2A''$	3.297	1.6952	0.1369	3.822	1.4258	0.1335

composed out of π-like FMOs) are intense, whereas the $\psi_-(\pi) \rightarrow \psi_+(\mathrm{lp})$ and $\psi_-(\pi) \rightarrow \psi_-(\mathrm{lp})$ transitions are weak. Analogously to the stacked uracil dimer, in the methylated dimer cation spectrum at the vertical geometry, we expect at least three intense peaks: at 0.41, 1.45, and 3.27 eV. The former peak is the CR band, and the latter two are the local excitations (LE) involving other π-like DMOs, i.e., the $\psi_+(\mathrm{lp(O)} + \mathrm{lp(N)})$ and $\psi_-(\mathrm{lp(N)} + \pi_{CC} + \pi_{CO})$. The transition dipole moment is related to $s_{\nu_{F_1}\nu_{F_2}}$, the overlap of the FMOs on fragments 1 and 2, by the following equation:

$$I(\psi_-(\nu) \rightarrow \psi_+(\nu)) \propto \frac{R_{AB}}{\sqrt{1 - s_{\nu_{F_1}\nu_{F_2}}}} \qquad (2)$$

where R_{AB} is the interfragment distance.

Upon the geometry relaxation, the states of the dimer become more delocalized, as can be seen in Figure 5 showing the two highest-occupied DMOs at the neutral and cation geometries. The states derived from the $\mathrm{lp(O_1)}$ and $\mathrm{lp(O_2)}$ FMOs are no longer localized on one of the fragments, as they were at the vertical geometry (not shown). Thus, we expect the following changes in the spectrum. The increasing overlap between the $\psi_+(\pi_{CC})$ and $\psi_-(\pi_{CC})$ DMOs leads to the growth of the intensity of the CR band, which shifts to 1.48 eV upon the relaxation.

TABLE 5: Ionization Energies (eV) and the DMO Character[a] Corresponding to the 10 Lowest Ionized States of the Stacked 1,3-Dimethyluracil Dimer at the Vertical Geometry (Isomer 1) Calculated at the IP-CCSD/6-31(+)G* Level[b]

	neutral		cation	
state	DMO	IE	DMO	E_{ex}
X^2A_1	$\psi_-(\pi_{CC})$	8.40 (−0.63)	$\psi_-(\pi_{CC})$	0.00
1^2A_1	$\psi_+(\pi_{CC})$	8.81 (−0.75)	$\psi_+(\pi_{CC})$	1.48
2^2A_1	ψ_-(lp(O) + lp(N))	9.42 (−0.96)	ψ_-(lp(O) + lp(N))	1.99
3^2A_1	lp(O_1), F1	9.66 (−0.40)	ψ_-(lp(O_1))	2.16
4^2A_1	lp(O_1), F2	9.69 (−0.43)	ψ_+(lp(O_1))	2.19
5^2A_1	ψ_+(lp(O) + lp(N))	9.85 (−0.59)	ψ_+(lp(O) + lp(N))	2.41
6^2A_1	lp(O_2), F1	10.46 (−0.48)	ψ_-(lp(O_1))	3.07
7^2A_1	lp(O_2), F2	10.51 (−0.48)	ψ_+(lp(O_1))	3.09
8^2A_1	ψ_-(lp(N) + π_{CC} + π_{CO})	11.67 (−0.94)	ψ_-(lp(N) + π_{CC} + π_{CO})	4.26
9^2A_1	ψ_+(lp(N) + π_{CC} + π_{CO})	11.88 (−1.00)	ψ_+(lp(N) + π_{CC} + π_{CO})	4.37

[a] In the DMO-LCFMO notations,[21] $\psi_+(\nu)$ and $\psi_-(\nu)$ represent the bonding and antibonding combinations of the MOs of fragments 1 and 2 (ν_{F1} and ν_{F2}). [b] The shifts of IEs (eV) of the dimethylated uracil dimer relative to the non-methylated analogue are given in parentheses. For the relaxed cation, the excitation energies (eV) calculated at the IP-CCSD/6-31(+)G* level are presented.

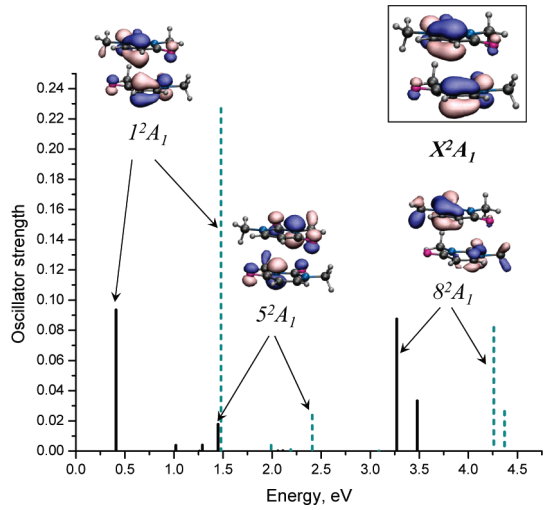

Figure 11. The three most intense transitions in the electronic spectrum of the lowest isomer of stacked 1,3-dimethyluracil cation at vertical (solid black) and cation (dashed blue) geometries. The DMOs corresponding to the ground state (framed) and excited states (regular) are shown. The positions of the peaks were calculated at the IP-CCSD/6-31(+)G* level, while the intensities are from the non-methylated dimer calculations.

On the basis of the similarity of the methylated and non-methylated systems, we expect the intensity of the CR band to (at least) double at the relaxed geometry. The position of the LE band that appears at 1.45 eV at the vertical geometry shifts to 2.41 eV; however, as follows from the FMO overlaps and splittings, no considerable increase of intensity is expected. Finally, the LE transition at 3.27 eV in the vertical spectrum shifts by +1.0 eV and its intensity decreases upon relaxation.

4. Conclusions

The structures, binding energies, and properties of several isomers of the neutral and ionized 1,3-dimethylated uracil dimers are characterized using *ab initio* methods. The methylation suppresses the formation of hydrogen-bonded and t-shaped neutral structures; however, the π-stacked manifold is rather dense. Five lowest isomers of the stacked dimer lie within the 2.9 kcal/mol range, which suggests that all of the isomers will be present at the standard conditions. The binding energies of the neutral dimers are in the range 10.9−13.8 kcal/mol (DFT-D). Surprisingly, in sterically constrained and less polar methylated species, the fragments are bound stronger than in the non-methylated analogues (the corresponding DFT-D estimate for the stacked uracil dimer is 10.5 kcal/mol).

The MOs of the uracil are only slightly perturbed by the CH_3 group; however, the effect is significant for the values of IEs. The methylation lowers the first IE of the 1,3-dimethyluracil by 0.6 eV as compared to uracil; the higher-lying states also exhibit red shifts of a varying magnitude (0.37−0.86 eV). This IE lowering is due to the electron-donating CH_3 groups, which increase the electron density in the ring and stabilize the ionized state. The effect is greater in the states derived from ionization from the delocalized π-orbitals, in which the electron density is efficiently donated to the π-system via the lp(N) component. The magnitude of the effect correlates with the weight of lp(N) in the leading MO, which is not surprising as nitrogens are the primary substitution sites.

Similarly to the uracil dimer, the electronic structure of the methylated uracil dimer is well described by DMO-LCFMO. The stacking interactions lower the first IE by 0.37 eV in the methylated dimers, which is very similar to 0.35 eV lowering in the non-methylated system (and the stacked dimer of thymine). Another important finding is the 0.6 eV lowering of the IE in the methylated dimer due to the methylation: the effect is the same as in the monomer. It implies that the effect of substitutions can be incorporated into the qualitative DMO-LCFMO picture as a constant shift of the dimer and monomer levels, whereas the splittings between the in-phase and out-of-phase DMOs are surprisingly insensitive to the substitution, except for the states derived from orbitals with large weights of lp(N). These states exhibit much larger splittings than in non-methylated species (i.e., 0.43 vs 0.06 eV), which ultimately results in changes in the ordering of the states. This is different from other model systems that we have studied (benzene, uracil, and adenine dimers) where the stacking interactions do not change the relative order of the ionized states, even though the splittings in different pairs of states are quite different.

Ionization changes the bonding pattern, inducing considerable changes in structures and binding energies. The energy separation between the isomers increases, so one can expect a dominant population of the lowest isomer at the standard conditions. The binding energies increase 1.4−2.0 fold upon ionization and lie in the 17.9−28.0 kcal/mol range (DFT-D); for the lowest-energy dimer cation structure, the IP-CCSD value of D_e is 31.9 kcal/mol. This binding energy is larger than that in the non-methylated uracil and thymine dimers. Similarly to the neutrals, the methylation increases the interfragment interaction in the dimer.

The relaxation of the cation structures is governed by two distinct mechanisms: the hole delocalization (and the FMO overlap) and the electrostatic stabilization (interaction of the lp(O) with the localized hole).

Finally, we presented electronic spectra of the ionized species. Significant changes in the spectra upon relaxation can be exploited to monitor the ionization-induced dynamics in dimethylated uracils. At the vertical geometry, there are three intense transitions: at 0.41, 1.45, and 3.27 eV, the CR band at 0.41 eV and LE at 1.45 eV being the most intense. Upon relaxation, these bands are blue-shifted, and their intensities change to 1.48 (CR), 2.41 (LE), and 4.26(LE) eV. The CR band at 1.48 eV is expected be the most intense and can be used to monitor the relaxed stacked dimer cation formation.

Acknowledgment. We are grateful to Dr. Ksenia Bravaya for her insightful remarks and critical reading of the manuscript. This work was conducted in the framework of the *i*OpenShell Center for Computational Studies of Electronic Structure and Spectroscopy of Open-Shell and Electronically Excited Species (iopenshell.usc.edu) supported by the National Science Foundation through the CRIF:CRF CHE-0625419 + 0624602 + 0625237 grant, and is also supported by the CHE-0616271 grant.

Supporting Information Available: Tables showing the optimized geometries of neutral and ionized 1,3-dimethyluracil and stacked 1,3-dimethyluracil dimers, as well as the relevant energies. This material is available free of charge via the Internet at http://pubs.acs.org.

References and Notes

(1) Nir, E.; Kleinermanns, K.; de Vries, M. S. *Nature* **2000**, *408*, 949.
(2) Sponer, J.; Leszczynski, J.; Hobza, P. *Biopolymers* **2002**, *61*, 3.
(3) Saigusa, H. *Photochem. Photobiol.* **2006**, *7*, 197.
(4) de Vries, M. S.; Hobza, P. *Annu. Rev. Phys. Chem.* **2007**, *58*, 585.
(5) de Vries, M. S. In *Radiation induced molecular phenomena in nucleic acids*; Shukla, M., Leszczynski, J., Eds.; Springer: Berlin, 2008; p 323.
(6) Golubeva, A. A.; Krylov, A. I. *Phys. Chem. Chem. Phys.* **2009**, *11*, 1303.
(7) Zadorozhnaya, A. A.; Krylov, A. I. *J. Chem. Theory Comput.*, submitted for publication, **2009**.
(8) Bravaya, K. B.; Kostko, O.; Ahmed, M.; Krylov, A. I. *Phys. Chem. Chem. Phys.* DOI: 10.1039/b919930f.
(9) Kostko, O.; Bravaya, K. B.; Krylov, A. I.; Ahmed, M. *Phys. Chem. Chem. Phys.*, submitted for publication, **2009**.
(10) Müller-Dethlefs, K.; Hobza, P. *Chem. Rev.* **2000**, *100*, 143.
(11) Kratochvíl, M.; Engkvist, O.; Vacek, J.; Jungwirth, P.; Hobza, P. *Phys. Chem. Chem. Phys.* **2000**, *2*, 2419.
(12) Kabeláč, M.; Hobza, P. *J. Phys. Chem. B* **2001**, *105*, 5804.
(13) Kabeláč, M.; Hobza, P. *Chem.—Eur. J.* **2001**, *7*, 2067.
(14) Plützer, C.; Hünig, I.; Kleinermanns, K. *Phys. Chem. Chem. Phys.* **2003**, *5*, 1158.
(15) Satzger, H.; Townsend, D.; Stolow, A. *Chem. Phys. Lett.* **2006**, *430*, 144.
(16) He, Y.; Wu, C.; Kong, W. *J. Phys. Chem. A* **2004**, *108*, 943.
(17) Mulliken, R. S.; Person, W. B. *Molecular Complexes*; Wiley-Interscience: 1969.
(18) Badger, B.; Brocklehurst, B. *Trans. Faraday Soc.* **1969**, *65*, 2576.
(19) Badger, B.; Brocklehurst, B. *Trans. Faraday Soc.* **1969**, *65*, 2582.
(20) Badger, B.; Brocklehurst, B. *Trans. Faraday Soc.* **1969**, *65*, 2588.
(21) Pieniazek, P. A.; Krylov, A. I.; Bradforth, S. E. *J. Chem. Phys.* **2007**, *127*, 044317.
(22) Pieniazek, P. A.; Bradforth, S. E.; Krylov, A. I. *J. Chem. Phys.* **2008**, *129*, 074104.
(23) Pieniazek, P. A.; VandeVondele, J.; Jungwirth, P.; Krylov, A. I.; Bradforth, S. E. *J. Phys. Chem. A* **2008**, *112*, 6159.
(24) Pieniazek, P. A.; Sundstrom, E. J.; Bradforth, S. E.; Krylov, A. I. *J. Phys. Chem. A* **2009**, *113*, 4423.
(25) Pieniazek, P. A.; Arnstein, S. A.; Bradforth, S. E.; Krylov, A. I.; Sherrill, C. D. *J. Chem. Phys.* **2007**, *127*, 164110.
(26) Sinha, D.; Mukhopadhyay, D.; Mukherjee, D. *Chem. Phys. Lett.* **1986**, *129*, 369.
(27) Pal, S.; Rittby, M.; Bartlett, R. J.; Sinha, D.; Mukherjee, D. *Chem. Phys. Lett.* **1987**, *137*, 273.
(28) Stanton, J. F.; Gauss, J. *J. Chem. Phys.* **1994**, *101*, 8938.
(29) Nooijen, M.; Bartlett, R. J. *J. Chem. Phys.* **1995**, *102*, 3629.
(30) Golubeva, A. A.; Pieniazek, P. A.; Krylov, A. I. *J. Chem. Phys.* **2009**, *130*, 124113.
(31) Iikura, H.; Tsuneda, T.; Yanai, T.; Hirao, K. *J. Chem. Phys.* **2001**, *115*, 3540.
(32) Baer, R.; Neuhauser, D. *Phys. Rev. Lett.* **2005**, *94*, 043002.
(33) Chai, J.-D.; Head-Gordon, M. *J. Chem. Phys.* **2008**, *128*, 084106.
(34) Chai, J.-D.; Head-Gordon, M. *Phys. Chem. Chem. Phys.* **2008**, *10*, 6615.
(35) Grimme, S. *J. Comput. Chem.* **2004**, *25*, 1463.
(36) Hehre, W. J.; Ditchfield, R.; Pople, J. A. *J. Chem. Phys.* **1972**, *56*, 2257.
(37) Dunning, T. H. *J. Chem. Phys.* **1989**, *90*, 1007.
(38) Krishnan, R.; Binkley, J. S.; Seeger, R.; Pople, J. A. *J. Chem. Phys.* **1980**, *72*, 650.
(39) Shao, Y.; Molnar, L. F.; Jung, Y.; Kussmann, J.; Ochsenfeld, C.; Brown, S.; Gilbert, A. T. B.; Slipchenko, L. V.; Levchenko, S. V.; O'Neil, D. P.; Distasio, R. A., Jr.; Lochan, R. C.; Wang, T.; Beran, G. J. O.; Besley, N. A.; Herbert, J. M.; Lin, C. Y.; Van Voorhis, T.; Chien, S. H.; Sodt, A.; Steele, R. P.; Rassolov, V. A.; Maslen, P.; Korambath, P. P.; Adamson, R. D.; Austin, B.; Baker, J.; Bird, E. F. C.; Daschel, H.; Doerksen, R. J.; Drew, A.; Dunietz, B. D.; Dutoi, A. D.; Furlani, T. R.; SGwaltney. R.; Heyden, A.; Hirata, S.; Hsu, C.-P.; Kedziora, G. S.; Khalliulin, R. Z.; Klunziger, P.; Lee, A. M.; Liang, W. Z.; Lotan, I.; Nair, N.; Peters, B.; Proynov, E. I.; Pieniazek, P. A.; Rhee, Y. M.; Ritchie, J.; Rosta, E.; Sherrill, C. D.; Simmonett, A. C.; Subotnik, J. E.; Woodcock, H. L., III; Zhang, W.; Bell, A. T.; Chakraborty, A. K.; Chipman, D. M.; Keil, F. J.; Warshel, A.; Herhe, W. J.; Schaefer, H. F., III; Kong, J.; Krylov, A. I.; Gill, P. M. W.; HeadGordon, M. *Phys. Chem. Chem. Phys.* **2006**, *8*, 3172.
(40) Jurečka, P.; Šponer, J.; Černý, J.; Hobza, P. *Phys. Chem. Chem. Phys.* **2006**, *8*, 1985.
(41) Sinnokrot, M. O.; Sherrill, C. D. *J. Phys. Chem. A* **2003**, *107*, 8377.
(42) Sinnokrot, M. O.; Sherrill, C. D. *J. Am. Chem. Soc.* **2004**, *126*, 7690.

JP910440D